Progress in Natural Science: Materials International 27 (2017) 74–80

Contents lists available at ScienceDirect

Progress in Natural Science: Materials International

journal homepage: www.elsevier.com/locate/pnsmi

Original Research

$MgCo_2$-D_2 and MgCoNi-D_2 systems synthesized at high pressures and interaction mechanism during the HDDR processing

Chubin Wan[a,b], V.E. Antonov[c], R.V. Denys[b,d], V.I. Kulakov[c], V.A. Yartys[b,e,*]

[a] University of Science and Technology Beijing, 100083, China
[b] Institute for Energy Technology, P.O. Box 40, Kjeller NO-2027, Norway
[c] Institute of Solid State Physics, Russian Academy of Sciences, Chernogolovka 142432, Russia
[d] HYSTORSYS AS, P.O. Box 45, Kjeller NO-2027, Norway
[e] Norwegian University of Science and Technology, Trondheim NO-7491, Norway

ARTICLE INFO

Keywords:
Intermetallics
Hydrogen storage materials
Neutron powder diffraction
High pressure synthesis
Phase-structural transformations
Magnesium
Cobalt
Nickel

ABSTRACT

$MgCo_2$ and MgNiCo crystallize with hexagonal Laves type intermetallic structures of the C14 type and do not form hydrides at ambient hydrogen pressures. However, applying high hydrogen pressures in the GPa range forces the hydrogen absorption and leads to the formation of multi-phase compositions, which contain approximately 2.5 atoms H per formula unit of $MgCo_2$ or MgNiCo and remain thermally stable under normal conditions.

The hydrogenation of $MgCo_2$ resulted in its decomposition to a ternary Mg_2CoD_5 deuteride and metallic cobalt. Phase-structural transformations accompanying the vacuum desorption of deuterium in the temperature range of 27–500 °C were studied using *in situ* neutron powder diffraction. The investigation showed a complete recovery of the initial $MgCo_2$ intermetallic *via* a Hydrogenation-Disproportionation-Desorption-Recombination process. At 300 °C, the Mg_2CoD_5 deuteride first decomposed to elementary Mg and hexagonal Co. At 400 °C, a MgCo phase was formed by interaction between Mg and Co. At the highest processing temperature of 500 °C, a solid-state interaction of MgCo and Co resulted in the recovery of the initial $MgCo_2$.

The interaction of MgNiCo with deuterium under the synthesis conditions of 2.8 GPa and 200 °C proceeded in a more complex way. A very stable ternary deuteride $MgNi_2D_3$ was leached away while Co was separated in the form of Mg_2CoD_5 and the remaining nickel formed a solid solution with Co with the approximate composition $Ni_{0.7}Co_{0.3}$.

The thermal desorption of deuterium from $MgCo_2D_{2.5}$ and from $MgNiCoD_{2.5}$ has been studied by Thermal Desorption Spectroscopy with deuterium released into a closed volume. The observed effects nicely correlate with changes in the phase structural composition of the hydrides formed.

$MgCo_2$ is a new example of the hydrogen storage alloy, in which a successful HDDR processing results in the reversible formation of the initial intermetallic at much lower temperatures than in the equilibrium phase diagram of the Mg-Co system.

1. Introduction

Cost- and performance-efficient hydrogen storage is required for the broad implementation of zero-emission hydrogen-based energy technologies. The advantages of Mg-based materials for the reversible hydrogen storage include large H storage capacity of MgH_2 – 7.6 mass % H, abundance of magnesium in the earth's crust, and low cost of Mg metal [1,2]. Compared to the individual MgH_2 hydride, the transition metal-containing Mg-based Mg_2FeH_6, Mg_2CoH_5 and Mg_2NiH_4 ternary hydrides maintain relatively high gravimetric (5.5, 4.5 and 3.6 wt% H) and volumetric (150, 125 and 97 g H/L) hydrogen storage capacities while offering advantages of decreased thermal stability caused by the modifications of the thermodynamics of the metal-hydrogen interactions [3,4].

In the Mg-Co-H system, two ternary hydrides have previously been synthesized and characterized. These are the γ-$Mg_6Co_2H_{11}$ hydride with an orthorhombic crystal structure [5,6] and the Mg_2CoH_5 hydride [7,8] forming two modifications. The low-temperature β-Mg_2CoH_5 modification has a tetragonal structure (space group *P4/nmm*; *a*=0.4480; *c*=0.6619 nm at room temperature) [7]; it reversibly trans-

Peer review under responsibility of Chinese Materials Research Society.
* Corresponding author.
E-mail address: volodymyr.yartys@ife.no (V.A. Yartys).

http://dx.doi.org/10.1016/j.pnsc.2017.01.007
Received 1 October 2016; Accepted 30 November 2016
Available online 04 February 2017

forms into the high-temperature modification γ-Mg_2CoH_5 with a disordered cubic structure at the temperature around 215 °C [5,7].

The Mg-Co based hydrides were synthesized by high temperature sintering [5,6,9] and ball milling [5,10]. Despite $MgCo_2$ is the only stable intermetallic compound existing in the Mg-Co system [11,12], thermodynamically metastable MgCo [9] and Mg_2Co [3,11] compounds can also be formed during the thermal decomposition of Mg_2CoH_5. The existence of the Mg_2Co phase was first reported by Ivanov [5], and subsequent investigations provided evidence that this compound is in fact formed at different Mg/Co ratios, as Mg_2Co [10,13,14] and as MgCo [6,9].

Gennari et al. [15] found that the formation of the MgCo and $MgCo_2$ phases depends on the synthesis conditions. Indeed, using the temperatures below 450 °C favors the formation of MgCo; heating to the temperatures near 500 °C causes the formation of $MgCo_2$ owing to the increased diffusion rates, and these two phases coexist at intermediate temperatures between 450 and 500 °C.

Norek et al. [16] investigated the synthesis and thermal decomposition of Mg_2CoH_5 by using *in situ* synchrotron powder X-ray diffraction and observed that Mg_2CoH_5 decomposed into elementary Mg and Co at 300 °C, while MgCo intermetallic was formed at 400 °C. Verón et al. [17] studied the thermodynamic behavior of the milled Mg-Co-H system and characterized the thermodynamic stabilities of $Mg_6Co_2H_{11}$ and Mg_2CoH_5 as being similar to each other.

In our earlier studies [18,19], a $MgNi_2H(D)_3$ trihydride was synthesized at 300 °C at high hydrogen (deuterium) pressures using $H_2(D_2)$ gas compressed to 2.8–7.4 GPa. The hydrogen-induced phase transformation from the C36 Laves-type structure of $MgNi_2$ to an orthorhombic $MoSi_2$-type related structure of $MgNi_2D_3$ took place. In the crystal structure of $MgNi_2D_3$, deuterium atoms occupy two types of interstices, inside the Mg_4Ni_2 octahedra and within the buckled nickel nets.

While the individual $MgNi_2$ intermetallic alloy crystallizes with the C36 Laves-type structure [18,20,21], the crystal structure of $MgCo_2$ is of the $MgZn_2$ C14 Laves type [20]. Thus, it can be envisaged that a gradual change of the Co/Ni ratio within the quasi-binary compositions $Mg(Ni_{1-x}Co_x)_2$ (x=0–1) could be accompanied by interesting changes in both structural and hydrogenation behaviors.

In the present study, $MgCo_2$ and MgNiCo intermetallic alloys were loaded with deuterium under a D_2 pressure of 2.8 GPa at 200 °C and at room temperature. Phase identification in the resultant Mg-Co-D and Mg-Ni-Co-D compositions was performed by X-ray diffraction. The thermal stability and the total deuterium content of these compositions were probed by Thermal Desorption Spectroscopy (TDS). In order to establish the mechanism of the phase-structural transformations in the $MgCo_2$-D_2 system, the deuterium desorption from a massive $MgCo_2$-D sample was studied by *in situ* neutron powder diffraction in the temperatures range from 27 to 500 °C. We did not observe any significant difference in the phase composition or deuterium desorption from the samples synthesized at 200 °C and at room temperature. For certainty, we will further refer to the results obtained with the 200 °C samples only.

2. Experimental

The $MgNi_xCo_{2-x}$ (x=0 and 1) intermetallic compounds were prepared from the mixtures of Mg, Ni and Co powders with the purity higher than 99.8%. An excess of 2% Mg was added to the stoichiometric compositions in order to compensate for its evaporation during the high temperature synthesis. The mixtures were compacted into pellets at a pressure of 25 MPa, wrapped into a Ta foil and placed into stainless steel tubes. The tubes were sealed by welding in Ar, annealed at 800 °C for 24 h and quenched together with the pellets into iced water. The pellets thus prepared were examined by X-ray diffraction (XRD) with a Siemens D500 diffractometer using Cu-Kα radiation.

To prepare the $MgCo_2$- and MgNiCo-based hydrides, approx. 200 mg of the intermetallic alloy were powdered in an agate mortar and loaded with deuterium by a 24 h exposure to a D_2 pressure of 2.8 GPa at 200 °C for 24 h followed by rapid cooling (quenching) to 100 K. The experiments were carried out in a "lentil" type high-pressure chamber [22] using AlD_3 as an internal deuterium source. The hydrogenation method is described in more detail elsewhere [23]. The synthesized samples were then stored in liquid nitrogen to prevent deuterium losses and oxidation by air.

The 1000 mg sample of deuterated $MgCo_2$ for the neutron diffraction study was collected in a few successive runs of high-pressure syntheses at 2.8 GPa and 200 °C. In view of the small protium concentration H/(H+D)=2.9(2) at% in the AlD_3 powder [24], which produced the D_2 gas in these experiments, we neglected the H contamination of the obtained $MgCo_2$-D sample in the analysis of its neutron diffraction patterns.

Each deuterated sample was examined by X-ray diffraction at 85 K with a Siemens D500 diffractometer using Cu Kα radiation selected by a diffracted beam monochromator. The diffractometer was equipped with a home-designed nitrogen cryostat that permitted the samples to be loaded without any intermediate warming.

The thermal stability and the total deuterium content of the samples were determined by hot extraction into a pre-evacuated calibrated volume, which involved heating the sample from −186 to 450 °C at a rate of 10 °C min^{-1}. The mass of the analyzed probe was a few milligrams. The method is described in more detail in Ref. [18].

In situ neutron powder diffraction (NPD) studies were performed at SINQ neutron source, Paul Scherrer Institute, Switzerland, using the HRPT Diffractometer [25] in the high intensity mode (λ=1.494 Å, 2θ range 3.85–164.75°, step 0.05°). The deuterated sample was loaded into a stainless steel autoclave with a valve allowing its connection to the gas/vacuum line during the *in situ* measurements. All reloading operations were performed in high-purity Ar atmosphere.

The temperatures of up to 500 °C desired for the NDP studies were achieved using a standard radiation type furnace. During the measurements, the interior of the furnace was continuously evacuated with a turbomolecular pump, thus protecting the tantalum heating elements from oxidation. The temperature was controlled with an accuracy of at least 0.1 K. The measurements were performed under two types of testing conditions. In one set of experiments, the sample was heated in a closed autoclave filled with argon and equilibrated (for at least 4 h) at five setpoint temperatures of 27, 150, 200, 250, 300 °C. The initial Ar pressure was 1 bar. In the second set of experiments, the sample was subjected to the dynamic vacuum conditions and equilibrated at 300, 350, 400, 450, and 500 °C. In total, 10 data sets were collected in an overall period of 37 h of hold time were analyzed.

The powder diffraction data were analyzed by Rietveld profile refinements method using the General Structure Analysis System (GSAS) software [26].

3. Results and discussion

3.1. Mechanism of $MgCo_2$ and MgNiCo interaction with high pressure deuterium

According to the XRD analysis, both initial alloys are single phase C14 Laves type alloys with hexagonal unit cells. The unit cell parameters of $MgCo_2$ (a=4.85459(1), c=7.9412(2) Å) and MgNiCo (a=4.8367(1), c=7.8882(2) Å) well agree with the reference data [9,27] and show a small contraction of the unit cell (1.4% in volume) following a replacement of Co in $MgCo_2$ by Ni to form MgNiCo.

Both intermetallic alloys proved to disproportionate during their 24 h interaction with deuterium at 2.8 GPa and 200 °C. Interestingly, the disproportionation does not result in the formation of a binary magnesium hydride MgH_2. Instead, it leads to the formation of stable ternary magnesium-based hydrides containing cobalt and nickel.

Table 1
Crystallographic data for the phase constituents in $MgCo_2$-D system.

Temperature	Phases	Space group	Unit cell parameters		
			a, Å	c, Å	V, Å^3
27 °C	Co	$P6_3/mmc$	2.5071(1)	4.0764(5)	22.19(1)
	Mg_2CoD_5	$P4/nmm$	4.4683(5)	6.577(2)	131.31 (3)
	MgO	$Fm\bar{3}m$	4.2128(6)	–	74.77(3)
150 °C	Co	$P6_3/mmc$	2.5134(1)	4.0817(5)	22.33(1)
	Mg_2CoD_5	$P4/nmm$	4.4843(6)	6.593(2)	132.58(4)
	MgO	$Fm\bar{3}m$	4.2187(8)	–	75.08(4)
200 °C	Co	$P6_3/mmc$	2.5152(1)	4.0839(6)	22.38(1)
	Mg_2CoD_5	$P4/nmm$	4.5059(7)	6.581(2)	133.61(5)
	MgO	$Fm\bar{3}m$	4.2213(7)	–	75.22(4)
250 °C	Co	$P6_3/mmc$	2.5166(1)	4.0839(5)	22.42(1)
	Mg_2CoD_5	$Fm\bar{3}m$	6.4591(6)	–	269.47(7)
	MgO	$Fm\bar{3}m$	4.2248(7)	–	75.41(3)
300 °C	Co	$P6_3/mmc$	2.5182(1)	4.0889(5)	22.46(1)
	Mg_2CoD_5	$Fm\bar{3}m$	6.4754(6)	–	271.52(7)
	MgO	$Fm\bar{3}m$	4.2275(6)	–	75.55(3)
V-300 °C	Co	$P6_3/mmc$	2.5182(1)	4.0889(5)	22.46(1)
	Mg	$P6_3/mmc$	3.234(2)	5.252(2)	47.56(4)
	MgO	$Fm\bar{3}m$	4.2270(6)	–	75.53(3)
V-350 °C	Co	$P6_3/mmc$	2.5136(1)	4.1187(5)	22.54(3)
	Mg	$P6_3/mmc$	3.239(2)	5.260(5)	47.79(4)
	MgO	$Fm\bar{3}m$	4.2294(5)	–	75.66(3)
V-400 °C	Co	$P6_3/mmc$	2.516(3)	4.140(6)	22.70(5)
	Co	$Fm\bar{3}m$	3.555(2)	–	44.94(7)
	MgCo	$Fd\bar{3}m$	11.530(2)	–	1532.9(9)
	MgO	$Fm\bar{3}m$	4.2324(5)	–	75.82(3)
V-450 °C	Co	$P6_3/mmc$	2.522(3)	4.136(7)	22.79(6)
	Co	$Fm\bar{3}m$	3.558(2)	–	45.05(6)
	MgCo	$Fd\bar{3}m$	11.542(2)	–	1537.7(8)
	MgO	$Fm\bar{3}m$	4.2355(5)	–	75.99(3)
V-500 °C	Co	$P6_3/mmc$	2.523(4)	4.142(8)	22.83(8)
	Co	$Fm\bar{3}m$	3.560(2)	–	45.13(6)
	MgCo	$Fd\bar{3}m$	11.555(5)	–	1543(2)
	$MgCo_2$	$P6_3/mmc$	4.8952(8)	7.999(3)	165.99(5)
	MgO	$Fm\bar{3}m$	4.2394(4)	–	76.19(2)

The XRD study of the quenched samples makes it possible to establish the final products and therefore the mechanism of interaction. For $MgCo_2$, the deuteration process can be described by the following equation:

$$MgCo_2 + D_2 \rightarrow \beta\text{-}Mg_2CoD_5\,(38\ wt.\ \%) + \varepsilon\text{-}CoD_{0.07}(62\ wt.\ \%)$$

The atomic ratio D/Co≈0.07 of the hcp (ε) solid solution Co-D is roughly estimated from the deuterium-induced lattice expansion of hcp Co using results of Ref. [28] and agrees with the pressure dependence of hydrogen solubility in hcp Co determined in Ref. [29]. We omit a discussion of these results because a similar sample of deuterated $MgCo_2$ was thoroughly investigated by neutron diffraction at 27 °C and higher temperatures (see Section 3.3.1); the only difference was that the ε-$CoD_{0.07}$ solid solution had lost all hydrogen and transformed into the hcp Co metal already at 27 °C.

The crystallographic data of Mg_2CoD_5 and hcp-Co listed in Table 1 well agree with the reference data (Mg_2CoH_5: a=4.4832 Å, c=6.5966 Å; hcp-Co: a=2.5054 Å, c=4.0743 Å [16]).

Fig. 1 presents Rietveld fittings of the XRD patterns of the initial MgNiCo intermetallic alloy collected at room temperature (a) and of the quenched deuterated MgNiCo sample measured at 85 K (b). For the deuterated material, the refinements show the formation of four different phases: the low temperature tetragonal β-Mg_2CoD_5 (Sp.gr. $P4/nmm$; a=4.889(1) Å, c=6.465(3) Å), orthorhombic $MgNi_2D_3$, fcc $Ni_{0.7}Co_{0.3}$ alloy (Sp. gr. $Fm\bar{3}m$, a=3.527(1) Å) and hcp Co (Sp. gr. $P63/mmc$, a=2.506(3), c=4.05(1) Å). The crystallographic data for $MgNi_2D_3$ (Sp. gr. $Cmca$, a=4.590 Å, b=8.794 Å, c=4.686 Å) was taken from ref. [18], and the weight fraction of $MgNi_2D_3$ was only refined.

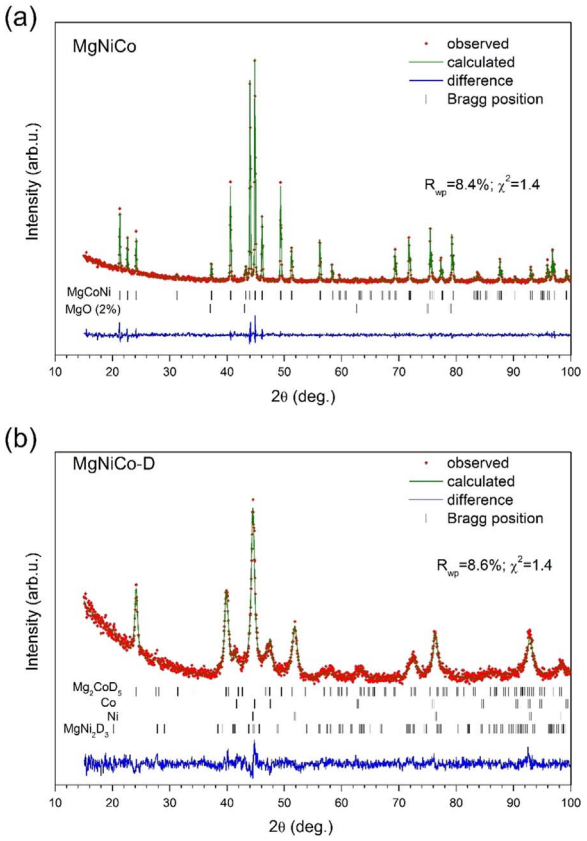

Fig. 1. X-ray diffraction patterns of (a) the initial MgCoNi alloy (room temperature, Cu $K\alpha_1$ radiation) and (b) a quenched sample of the alloy deuterated at 2.8 GPa and 200 °C (T=85 K, Cu Kα radiation).

The scheme of the hydrogenation process is presented below:

$$MgNiCo + D_2 \rightarrow Mg_2CoD_5(40wt.\ \%) + MgNi_2D_3(6\ wt.\ \%) + Ni_{0.7}Co_{0.3}(50wt.\ \%) + \varepsilon\text{-}Co\ (4wt.\ \%)$$

The formation of $Ni_{0.7}Co_{0.3}$ was suggested based on the mass balance considerations of Ni and Co between MgNiCo and the reaction products, and based on a good agreement between the data for the formed Ni-based solid solution and the reference data for the $Ni_{0.7}Co_{0.3}$ alloy [30].

3.2. Thermal decomposition of the hydrides formed by $MgCo_2$ and by MgNiCo

Desorption of deuterium from each quenched sample of deuterated $MgCo_2$ and MgNiCo alloys was studied by temperature programmed desorption (TPD) in a pre-evacuated calibrated volume in the regime of heating from −186 to 450 °C at a rate of 10 °C min^{-1}. Fig. 2 presents deuterium desorption plots for the $MgCo_2$–D and MgNiCo-D systems and shows the amount of the released deuterium and the rate of the corresponding mass loss.

As one can see from Fig. 2a, the $MgCo_2$-D sample starts releasing D_2 after heating to about −50 °C. At temperatures up to approx. 200 °C, the deuterium mostly evolves from the hcp $CoD_{0.07}$ phase, which decomposes to hcp Co metal. At temperatures higher than 200 °C, the decomposition of the Mg_2CoD_5 deuteride begins, and the rate of the

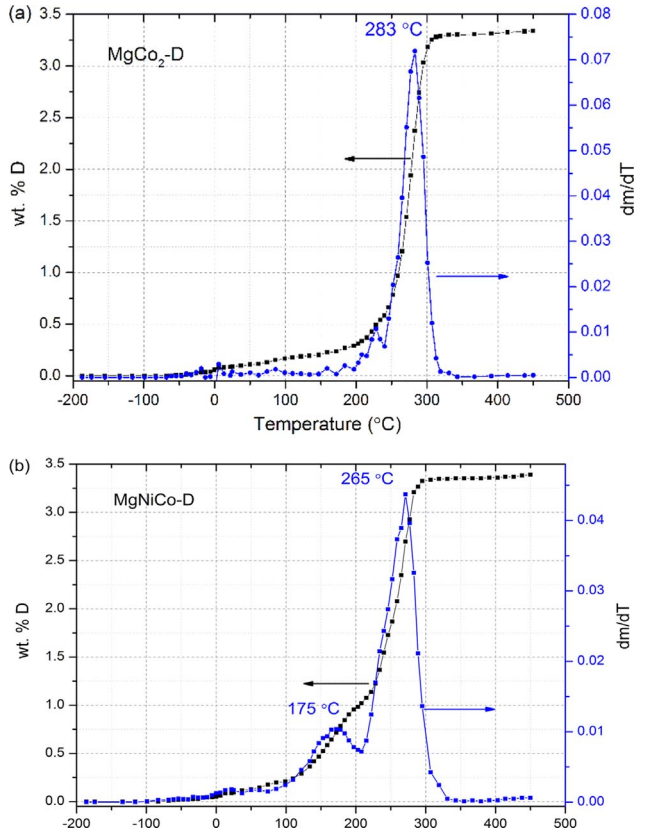

Fig. 2. Thermal desorption traces of the deuterium release (left scale, wt% D) and the rate of the mass loss (right scale, wt% D / K) measured in the regime of heating at a rate of 10 °C min^{-1} for the (a) $MgCo_2$-D and (b) MgNiCo-D quenched samples loaded with deuterium at 2.8 GPa and 200 °C.

decomposition reaches its maximum at approx. 283 °C. The total amount of the released deuterium is 3.34 wt% D.

As seen from Fig. 2b, the total content of deuterium of the MgNiCo-D samples was slightly higher and equal to 3.39 wt% D. Two different stages of the gas desorption were clearly demonstrated by the rate of the mass lost, dm/dT. The lower broad peak extending between approx. 100–200 °C with the maximum at 175 °C is mostly due to the decomposition of $MgNi_2D_3$ in agreement with [18]. The second broad peak observed between 200 and 300 °C with the maximum at 265 °C corresponds to the decomposition of Mg_2CoD_5. Compared to the $MgCo_2$-D samples, this peak is shifted to lower temperatures by approx. 20 °C.

Thus, the effect of Ni in $Mg(Ni,Co)_2$-D system is in decreasing the starting decomposition temperature and in shifting the desorption events to lower temperatures.

3.3. In situ *neutron powder diffraction study of the $MgCo_2$-D system*

3.3.1. *Experiments in argon gas (T=27–300 °C)*

In order to study phase-structural transformations in the $MgCo_2$-D system, the *in situ* NPD experiments were carried out in the regime of a step-wise heating of the sample in a temperature range between 27 and 500 °C. Initially, a stainless steel autoclave with the sample was filled with argon gas at a pressure of 1 bar. At 300 °C, the autoclave was evacuated and further experiments were performed in vacuum. Altogether we have measured 10 NPD data sets, five of which were collected under 1 bar of Ar at *T*=27, 150, 200, 250, 300 °C and then another five in vacuum at *T*=300, 350, 400, 450 and 500 °C. Each data set was measured for 4 min; the heating rate was 10 °C min^{-1}; the equilibration time was 4 h at each setpoint temperature before the measurement was started.

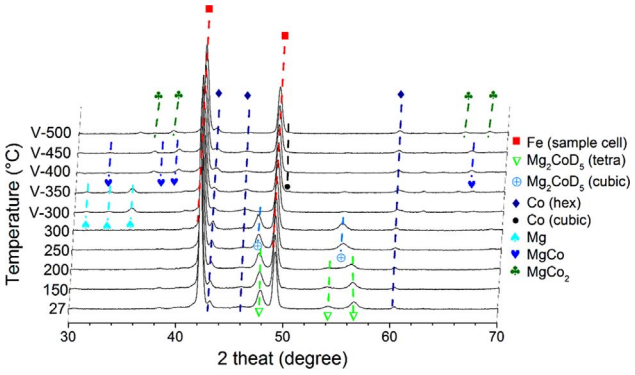

Fig. 3. *In situ* NPD patterns showing the evolution of the phase composition of the starting Mg_2CoD_5+ Co system. The sample was heated from 27 to 500 °C; the neutron wavelength was λ=1.494 Å. "V" stands for vacuum, otherwise – Ar gas at 1 bar.

In total, we identified the presence and refined the abundances of 7 phase constituents (further to the stainless steel sample cell and an impurity of MgO), including two modifications of Mg_2CoD_5 (low temperature (LT) tetragonal and high temperature (HT) cubic ones); two modifications of cobalt (LT hexagonal and HT cubic); Mg metal; MgCo and $MgCo_2$ intermetallic compounds.

Rietveld refinements for the starting data set of the deuterated $MgCo_2$ sample (T=27 °C, 1 bar of Ar) showed that it consists of two phases, the LT tetragonal β-Mg_2CoD_5 (23.9 wt%) and LT hexagonal Co (74.0 wt%); the indicated concentrations correspond to the mole ratio Mg_2CoD_5/Co≈1/6. A small amount of MgO (2.1 wt%) was also identified as an impurity. The disproportionation of $MgCo_2$ under high deuterium pressure established by X-ray diffraction (see Section 3.1) should have resulted in the mole ratio Mg_2CoD_5/Co≈1/3. The observed deficiency of Mg_2CoD_5 could be attributed to the presence of amorphous or poorly crystallized Mg_2CoD_5.

Fig. 3 shows the evolution of the *in situ* NPD patterns of the $MgCo_2$-D system with increasing temperature. As one can see, various reactions take place on heating. The evolution of the corresponding phase compositions derived from Rietveld refinements of the NPD data is shown in Fig. 4. The crystal structures of the identified phase constituents are listed in Supplementary material, Tables S1-S6, together with the Rietveld profile refinements plots of the NPD pattern for all studied samples and temperature conditions (Figs. S1-S9).

No changes of deuterium content took place in the temperature range 27–300 °C on heating in the closed autoclave. When the temperature rose to 250 °C, the tetragonal β-Mg_2CoD_5 (LT) phase

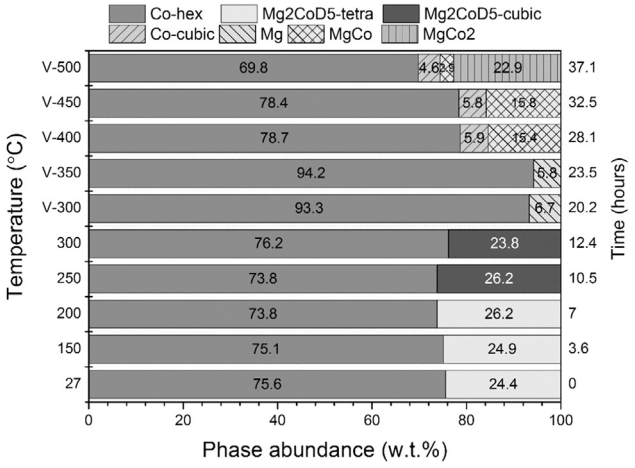

Fig. 4. Phase-structural transformations in the $MgCo_2$-D system from Rietveld refinements of the NPD data. The abundances of the phases are presented as a function of temperature and time during the heating of the $MgCo_2D_3$ sample synthesized at 2.8 GPa and 200 °C.

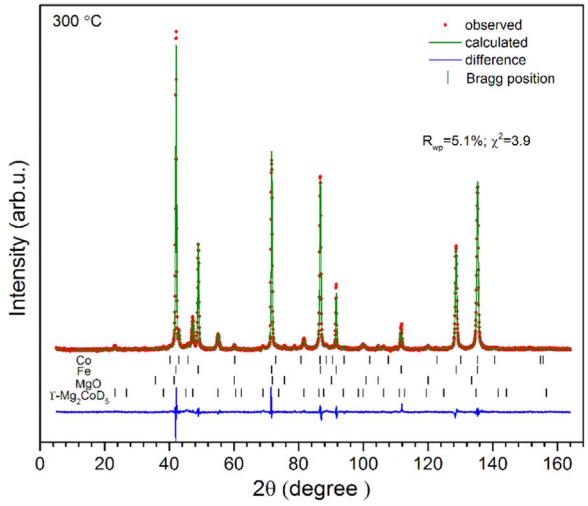

Fig. 5. *In situ* powder neutron diffraction pattern of the deuterated $MgCo_2$ sample at 300 °C under 1 bar Ar. Vertical bars show positions of the Bragg peaks of the identified phases: hexagonal Co; HT cubic γ-Mg_2CoD_5; Fe (from the sample cell) and MgO impurity.

transformed to its cubic modification γ-Mg_2CoD_5 (HT). This agrees with the observation of the allotropic transformation of LT β-Mg_2CoD_5 into the HT γ-Mg_2CoD_5 at about 215 °C reported earlier [7].

Fig. 5 shows the refined NPD pattern of the $MgCo_2D_3$ sample measured at 300 °C under 1 bar Ar. The sample was two-phase and contained the LT hexagonal phase of cobalt and the HT cubic modification of Mg_2CoD_5.

As shown in Fig. 4, the weight fractions of the Mg_2CoD_5 and Co phases remain almost unchanged when the sample is heated to 250 °C in Ar gas. At 300 °C, the amount of Mg_2CoD_5 starts decreasing (by approx. 2.3 wt%) and the amount of Co begins to increase. This is because Mg_2CoD_5 starts decomposing at this temperature rejecting magnesium. However, the magnesium metal is not yet visible in the reaction products due to its small amount and small grain size.

3.3.2. Processes taking place during deuterium desorption into vacuum at 300–500 °C

Bragg reflections from the mixture of γ-Mg_2CoD_5 and hexagonal Co are observed at temperatures up to 300 °C in the closed autoclave. After an exposure of the sample to the same temperature in vacuum, the diffraction peaks from the γ-Mg_2CoD_5 disappear that suggests a decomposition of this phase. The reaction is:

$$Mg_2CoD_5+3Co\rightarrow 2Mg+4Co+2.5\ D_2 \quad (1)$$

From the data presented in Fig. 4, it follows that the mole ratio of the Mg and Co phases is close to 1:5.7, which is small compared to the theoretical stoichiometry 1:2. This is likely to be due to sublimation of the Mg metal in vacuum. Besides, the mean crystallite sizes of Mg calculated using Scherrer Equation [25,31] are ~16 nm at both 300 and 350 °C. The sample obviously contains much smaller crystallites of Mg, which only contribute to the diffuse neutron scattering. This is another likely reason for the under stoichiometric content of Mg refined from the NPD data.

During further heating from 300 to 350 °C in vacuum, no changes are observed in the relative amounts of Mg and Co phases.

When the temperature increases to 400 °C, the MgCo compound is formed by depleting the Co content (~15.0 wt%) and by involving all available Mg (~6 wt%) into the chemical transformation. The solid-state reaction in the Mg-Co matrix is as follows:

$$Mg+Co\rightarrow MgCo \quad (2)$$

At 450 °C, no further changes happen in the sample. Our observations are in agreement with the results shown previously in [15,16,32,33].

According to Eq. (1), the amount of the MgCo product should exceed 20 wt%. However, its refined weight content is lower (~15.0 wt %), indicating that the MgCo compound has poor crystallinity. Indeed, MgCo forms very small crystallites the size of ~8.0 nm (calculations were performed using the Scherrer Equation).

In addition to the MgCo intermetallic, a small amount (~6 wt%) of the HT cubic-Co appears in the NPD patterns collected at 400 and 450 °C, as a result of phase transformation of the LT hexagonal Co to the HT cubic Co. The temperature of this allotropic transformation in Co

$$Co\text{-hexagonal}\rightarrow Co\text{-cubic} \quad (3)$$

well agrees with the reference data [15,16].

When the temperature increases to 500 °C, most of the crystalline MgCo phase vanishes, while $MgCo_2$ compound (22.5 wt%) is formed. Due to the stability of the MgCo compound at 500 °C [15], we can exclude a possibility of decomposition of MgCo to form a more stable $MgCo_2$ compound. This indicates that the solid-state interaction in the Co-rich alloys of the Mg-Co system can be described as.

$$MgCo+Co\rightarrow MgCo_2 \quad (4)$$

The amount of the formed $MgCo_2$ compound well agrees with the proposed scheme.

MgO impurity was present as an admixture phase from the very beginning. It almost kept a constant value at all studied temperature states, showing the absence of magnesium oxidation during the studied processing.

Table 1 summarizes results of the Rietveld refinements of NPD data for the $MgCo_2$-D system at various temperatures. The crystallographic data of the LT β-Mg_2CoD_5 phase at 27 °C agrees within narrow ranges with the reference data [7] of Mg_2CoD_5 at 25 °C. As seen from the data presented in Table 1, the unit cell of β-Mg_2CoD_5 experiences a small contraction (~−0.2%) in the [001] direction and small expansion (~+0.5%) along the [100] and [010] directions when heated above 150 °C. This means that the unit cell undergoes a distortion preceding the phase transformation. A similar distortion of the crystal structure was earlier observed in β-Mg_2CoH_5 near the point of allotropic transformation at 215 °C [4].

The volumes V_{LT} and V_{HT} per formula unit of the LT β-Mg_2CoD_5 and HT γ-Mg_2CoD_5 phases are presented in Fig. 6 as functions of temperature. As one can see, the coefficients of thermal expansion are considerably different for the LT and HT phases. The intersection of linear fits for the $V_{LT}(T)$ and $V_{HT}(T)$ dependences at a temperature

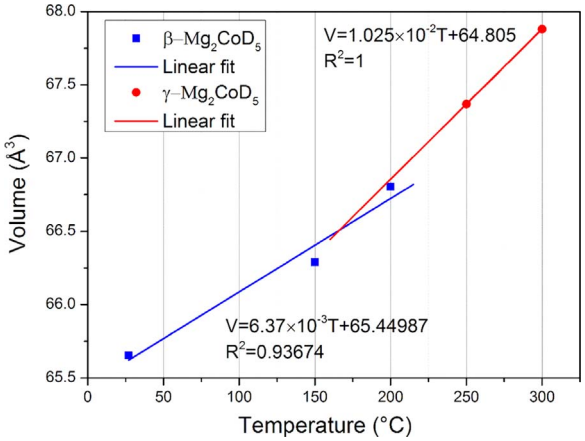

Fig. 6. Temperature dependences of the volumes per formula unit for the LT β-Mg_2CoD_5 and for the HT γ-Mg_2CoD_5.

much lower than T_0=215 °C established earlier for the LT→HT transformation [4] therefore confirms the positive volume effect of this transformation. At 215 °C, the fits give V_{LT} =66.819 and V_{HT}=67.009 Å^3. The difference V_{HT}–V_{LT}=0.19 Å^3, or 0.28% agrees with the volume increase of 0.26% accompanying the LT→HT transformation in Mg_2CoH_5 [4]. The subtle volume effect suggests that the transformation does not correlate with hydrogen release from the structure.

The linear fit of the V_{HT}(T) dependence in Fig. 6 gives V_{HT}(225 °C) =67.111 Å^3, which agrees with the experimental value V_{HT}(225 °C) =67.178 Å^3 determined for γ-Mg_2CoD_5 by Zolliker at al. [7].

Finally, it is of interest to compare some of the obtained results with the reference data for similar systems.

In an earlier report [9], a mixture of Mg and Co powders with the mean composition $Mg_{1.05}Co$ was compacted under 16 ton/cm^2 to form pellets and then sealed and heated to 350 °C (13 weeks), 400 °C (4 weeks) and 500 °C (2 weeks). An X-ray analysis showed that the MgCo phase with a cubic-structure (a=11.426 Å) was formed at 350 and 400 °C, while the $MgCo_2$ compound was observed in the 500 °C sample. In our work, the MgCo intermetallic phase could be produced in several hours at 400 and 450 °C in vacuum, but it did not form at a temperature as low as 350 °C. A possible reason is that our sample was only exposed to 350 °C for a very short time of about 4 h compared to 13 weeks in Ref. [9]. In this connection, the formation of the cubic MgCo phase at a relatively low temperature of 350 °C observed in [9] is likely to be a more equilibrium result.

Furthermore, the thermal stability of β-Mg_2CoD_5 proves to strongly depend on its synthesis conditions. In earlier reports, the decomposition of the Mg_2CoH_5 hydride occurred at 290–300 °C in the samples prepared by reactive mechanical alloying [15,32,34] and at a much higher temperature of 390–410 °C if the sample was sintered in a hydrogen gas [15,34,35]. In each case, the decomposition properties were characterized under a hydrogen pressure of 1 bar. The decomposition of Mg_2CoD_5 studied in the present work took place at 283 °C. We can therefore conclude that the decomposition performance of the sample obtained from the high-pressure D_2 synthesis is close to the properties of this hydride synthesized by reactive ball milling under the hydrogen gas. The increased interfacial area resulting from the RMA microstructural refinement is known to be critical for reducing the thermal stability of the hydride and for the corresponding decrease of its decomposition temperature [4]. Most likely, the lower decomposition temperature of the Mg_2CoD_5 deuteride in our experiments was due to the small grain size and high concentration of defects in the particles of this phase precipitated from the virgin $MgCo_2$ matrix during the high pressure synthesis.

4. Conclusions

In this work, we synthesized deuterides of $MgCo_2$ and MgNiCo Laves type intermetallic alloys by using high pressure synthesis at a pressure of 2.8 GPa and temperature of 200 °C.

In both cases, a disproportionation of the metal lattice takes place. The binary magnesium hydride is not formed as a product of the disproportionation. Instead, we observed the formation of one (Mg_2CoD_5 for $MgCo_2$) or two (Mg_2CoD_5 and $MgNi_2D_3$ for MgNiCo) ternary deuteride phases. Thus, the mechanism of interaction of the alloys with hydrogen becomes significantly affected by the transition metals, Co and Ni.

Time-resolved *in situ* neutron diffraction was employed to probe temperature-dependent phase-structural transformations in the $MgCo_2$-D system. We proposed mechanisms of decomposition of the Mg_2CoD_5 deuteride and the formation of Mg-Co compounds in the Co-rich part of the Mg-Co system and concluded that:

(a) The Mg_2CoD_5 deuteride decomposes into elementary Mg and Co at approximately 300 °C.
(b) An allotropic transformation from the LT tetragonal to the HT cubic modification of Mg_2CoD_5 takes place at around 250 °C.
(c) MgCo and $MgCo_2$ compounds are formed in the Mg-Co matrix by solid-state reactions at 400 and 500 °C, respectively.
(d) A formation of $MgCo_2$ after completion of the deuterium desorption shows that this Mg-Co intermetallic is a new example of the hydrogen storage alloy, for which a complete HDDR cycle was successfully accomplished.

Acknowledgements

This work is mainly based on the experiments performed at the Swiss spallation neutron source SINQ, Paul Scherrer Institute, Villigen, Switzerland. We are grateful to Dr. Denis Sheptyakov, Laboratory for Neutron Scattering and Imaging, Paul Scherrer Institute, for collecting the *in situ* NPD data for $MgCo_2D_{2.5}$.

This work was supported by the Norwegian Research Council (project “High Power Batteries Probed by Neutron Scattering”, program SYNKNØYT).

The work was financially supported by the National Natural Science Foundation of China (Grant No. 11605007). The first author acknowledges the funding project (No. 201506465019) by China Scholarship Council (CSC).

A support by a Grant of the Program on Elementary Particle Physics, Fundamental Nuclear Physics and Nuclear Technologies of RAS is also acknowledged.

Appendix A. Supporting information

Supplementary data associated with this article can be found in the online version at http://dx.doi.org/10.1016/j.pnsc.2017.01.007.

References

[1] H. Shao, G. Xin, J. Zheng, X. Li, E. Akiba, Nano Energy 1 (2012) 590–601.
[2] J.-C. Crivello, R.V. Denys, M. Dornheim, M. Felderhoff, D.M. Grant, J. Huot, T.R. Jensen, P. Jongh, M. Latroche, G.S. Walker, C.J. Webb, V.A. Yartys, Appl. Phys. A 122 (2016) 1–17.
[3] M.G. Verón, F.C. Gennari, G.O. Meyer, J. Power Sources 195 (2010) 546–552.
[4] G. Zepon, D.R. Leiva, M.J. Kaufman, S.J.A. Figueroa, R. Floriano, D.G. Lamas, A.A.C. Asselli, W.J. Botta, Int J. Hydrog. Energy 40 (2015) 1504–1515.
[5] E.Y. Ivanov, I.G. Konstanchuk, A.A. Stepanov, Y. Jie, M. Pezat, B. Darriet, Inorg. Chem. 28 (1989) 613–615.
[6] R. Černý, F. Bonhomme, K. Yvon, P. Fischer, P. Zolliker, D.E. Cox, A. Hewat, J. Alloy. Compd. 187 (1992) 233–241.
[7] P. Zolliker, K. Yvon, P. Fischer, J. Schefer, Inorg. Chem. 24 (1985) 4177–4180.
[8] P. Zolliker, K. Yvon, P. Fischer, J. Schefer, J. Less Common Met. 129 (1987) 211–212.
[9] M. Yoshida, F. Bonhomme, K. Yvon, P. Fischer, J. Alloy. Compd. 190 (1993) L45–L46.
[10] J. Chen, H.T. Takeshita, D. Chartouni, N. Kuriyama, T. Sakai, J. Mater. Sci. 36 (2001) 5829–5834.
[11] A.A. Nayeb-Hashemi, J.B. Clark, Bull. Alloy Phase Diagr. 8 (1987) 352–355.
[12] H.O.T. Massalski, P. Subramanian, L. Kacprzak, Binary Alloy Phase Diagrams, 2 ed, American Society for Metals, Metals Park, OH, 1990.
[13] J.-L. Bobet, S. Pechev, B. Chevalier, B. Darriet, J. Mater. Chem. 9 (1999) 315–318.
[14] T. Aizawa, K.-I. Hasehira, C. Nishimura, Mater. Trans. 44 (2003) 601–610.
[15] F.C. Gennari, F.J. Castro, J. Alloy. Compd. 396 (2005) 182–192.
[16] M. Norek, T.K. Nielsen, M. Polanski, I. Kunce, T. Płociński, L.R. Jaroszewicz, Y. Cerenius, T.R. Jensen, J. Bystrzycki, Int. J. Hydrog. Energy 36 (2011) 10760–10770.
[17] M.G. Verón, F.C. Gennari, J. Alloy. Compd. 614 (2014) 317–322.
[18] V.A. Yartys, V.E. Antonov, A.I. Beskrovnyy, J.C. Crivello, R.V. Denys, V.K. Fedotov, M. Gupta, V.I. Kulakov, M.A. Kuzovnikov, M. Latroche, Y.G. Morozov, S.G. Sheverev, B.P. Tarasov, Acta Mater. 82 (2015) 316–327.
[19] V.A. Yartys, V.E. Antonov, D. Chernyshov, J.C. Crivello, R.V. Denys, V.K. Fedotov, M. Gupta, V.I. Kulakov, M. Latroche, D. Sheptyakov, Acta Mater. 98 (2015) 416–422.
[20] K.H.J. Buschow, Magnetic properties of $MgCo_2$, $MgNi_2$ and Mg_2Ni, Solid State Commun. 17 (1975) 891–893.
[21] K.H.J. Buschow, P.G. van Engen, R. Jongebreur, J. Magn. Magn. Mater. 38 (1983) 1–22.
[22] L.G. Khvostantsev, V.N. Slesarev, V.V. Brazhkin, High Press. Res. 24 (2004) 371–383.
[23] V.E. Antonov, J. Alloy. Compd., 330 332 (2002) 110–116.

[24] V.E. Antonov, A.I. Davydov, V.K. Fedotov, A.S. Ivanov, A.I. Kolesnikov, M.A. Kuzovnikov, Phys. Rev. B 80 (2009) 134302.
[25] P. Fischer, G. Frey, M. Koch, M. Könnecke, V. Pomjakushin, J. Schefer, R. Thut, N. Schlumpf, R. Bürge, U. Greuter, S. Bondt, E. Berruyer, Phys. B: Condens Matter 276–278 (2000) 146–147.
[26] A.C. Larson, R.B.V. Dreele. Los Alamos National Laboratory Report LAUR, 2004, pp. 86–748
[27] E.I. Gladyshevskii, P.I. Krypyakevych, M.Y. Teslyuk, O.S. Zarechnyuk, Y.B. Kuzma, Sov. Phys. Crystallogr. 6 (1961) 207–208.
[28] V.K. Fedotov, V.E. Antonov, T.E. Antonova, E.L. Bokhenkov, B. Dorner, G. Grosse, F.E. Wagner, J. Alloy. Compd. 291 (1999) 1–7.
[29] V.E. Antonov, I.T. Belash, V.Y. Malyshev, E.G. Ponyatovskii, Dokl. Akad. Nauk SSSR 272 (1983) 1147–1150.
[30] J. Bandyopadhyay, K.P. Gupta, Cryogenics (Guildf.) 17 (1977) 345–347.
[31] A.L. Patterson, Phys. Rev. 56 (1939) 978–982.
[32] I.G. Fernández, G.O. Meyer, F.C. Gennari, J. Alloy. Compd. 446–447 (2007) 106–109.
[33] I. González Fernández, F.C. Gennari, G.O. Meyer, J. Alloy. Compd. 462 (2008) 119–124.
[34] I.G. Fernández, G.O. Meyer, F.C. Gennari, J. Alloy. Compd. 464 (2008) 111–117.
[35] M.G. Verón, A.M. Condó, F.C. Gennari, Int. J. Hydrog. Energy 38 (2013) 973–981.